

Statistics of Electromigration Lifetime Analyzed Using a Deterministic Transient Model

Jun He* and Z. Suo#

*Intel Corporation, 5200 NE Elam Young Parkway, Hillsboro, Oregon 97124

#Division of Engineering and Applied Sciences, Harvard University, Cambridge, MA 02138

Abstract. The electromigration lifetime is measured for a large number of copper lines encapsulated in an organosilicate glass low-permittivity dielectric. Three testing variables are used: the line length, the electric current density, and the temperature. A copper line fails if a void near the upstream via grows to a critical volume that blocks the electric current. The critical volume varies from line to line, depending on line-end designs and chance variations in the microstructure. However, the statistical distribution of the critical volume (DCV) is expected to be independent of the testing variables. By contrast, the distribution of the lifetime (DLT) strongly depends on the testing variables. For a void to grow a substantial volume, the diffusion process averages over many grains along the line. Consequently, the void volume as a function of time, $V(t)$, is insensitive to chance variations in the microstructure. As a simplification, we assume that the function $V(t)$ is deterministic, and calculate this function using a transient model. We use the function $V(t)$ to convert the experimentally measured DLT to the DCV. The same DCV predicts the DLT under untested conditions.

INTRODUCTION

In recent years, the electromigration behavior in on-chip interconnect structures has been significantly affected by changes such as replacing aluminum with copper [1,2], replacing silica with low-permittivity dielectrics [3-5], removing shunts [6,7], and adding caps [8]. This paper studies a fatal failure mode in dual damascene copper lines. As electron flow drives copper atoms to drift in a line, a void forms at the upstream via, grows to a critical volume, and blocks the electron flow.

Figure 1 shows two micrographs taken after an electromigration test. The electric current drives atoms to drift away from the via in the lower-level copper line. The liner underneath the via blocks atomic diffusion from one level to the other. The flux divergence causes the voids. Figure 2 shows a similar structure tested with an opposite electric current direction, so that atoms drift away from the via in the upper-level copper line.

In an old generation of interconnect structures, the TiAl layers provided shunts, so that interconnects could be designed on the basis of a *steady state* [9-12]. As atoms drift downstream, a compressive stress field builds up in the line to balance the electron flow. In the steady state, the net atomic flux stops, and the void volume saturates. The line is immortal if the saturated void volume is below a critical value.

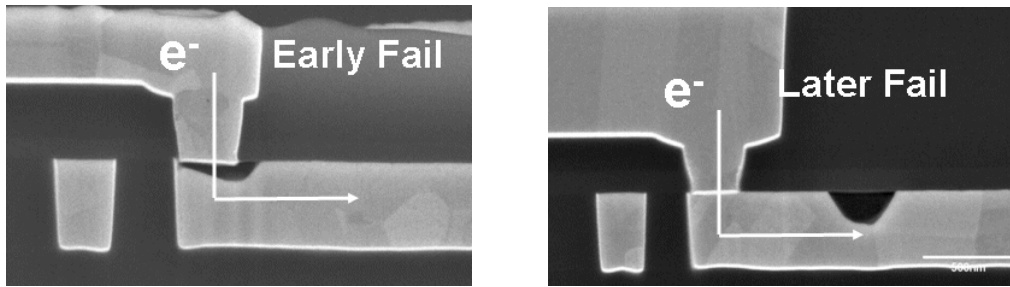


FIGURE 1. FIB cross sections of the dual damascene copper lines, cut along the length of the lines after electromigration testing. The liner underneath the via blocks the atomic diffusion between the copper lines at the two levels. The electric current drives atoms to drift away from the via in the lower-level line. (a) A void right beneath the via leads to an open-circuit failure early. (b) A void away from the via only causes a minor resistance increase; this line lasts longer.

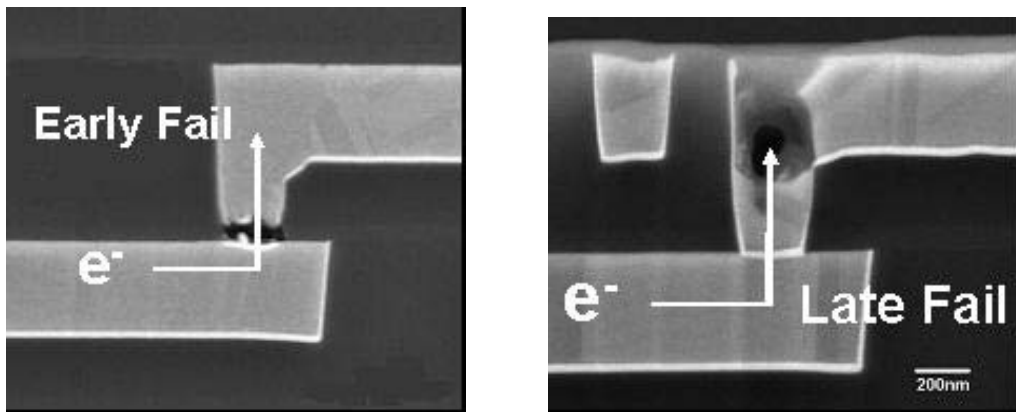


FIGURE 2. The electric current drives atoms to drift away from the via in the upper-level line. (a) A small void corresponds to an early fail. (b) A large void corresponds to a late fail.

Two factors make copper lines mortal under representative testing conditions. First, the liners now in use are not an effective current shunt, so that a relatively small void at the upstream via can block the electron flow and cause an abrupt increase in the electrical resistance. Second, the copper lines are embedded in an organosilicate glass, which is compliant, so that the saturated void volume is large.

The critical void volume varies from line to line, as illustrated in Figs. 1 and 2, as well as by others in the literature [1,2,4,6,7]. We develop a method to analyze lifetime data by a combination of this statistical variation and a deterministic transient model. Our method rests on two premises. First, the distribution of the critical volume (DCV) is independent of testing variables (i.e., the line length, the electric current density, and the temperature). Second, the functional relationship between the void volume and time, $V(t)$, is deterministic. The two premises idealize the following notions. The critical void volume is largely determined by the local geometry near the upstream via, and should be insensitive to the testing variables. For a void to grow to a substantial volume, the diffusion process has to average over many grains along the line, so that $V(t)$ should be insensitive to chance variations in the microstructure.

This paper ascertains the two premises by comparing their predictions to experimental data. The distribution of lifetime (DLT) is measured for a large number of copper lines under many testing conditions. The function $V(t)$ is calculated by using a transient model. We use the function $V(t)$ to obtain the DCV from the experimentally measured DLT under a few testing conditions. The same DCV predicts the DLT under other testing conditions.

MEASURED TIMES-TO-FAIL

We test copper lines of two designs, A and B. The two designs share the same material set and the same integration process. Consequently, all interfaces, as well as copper grain structures, should have no systematic variation from line to line. The via size and line cross section area in Design B is about 30% smaller than that of Design A. The integration process used here is speculative, resulting in large statistical variations in electromigration lifetime.

Figure 3 shows the cumulative percentage frequency of the time-to-fail, measured from 8 groups of copper lines of Design A, on a single wafer, at temperature 300C. Each group consists of 12-18 lines, picked uniformly across the wafer to capture process variation within the wafer. The line length L and the electric current density j are constant for each group of lines, but vary from group to group. The electric current drives atoms to drift away the via in the lower-level copper line (Fig. 1). Failure of a line is identified by an abrupt increase in the electric resistance. When either L or j is small, the time-to-fail has a large median and a wide dispersion.

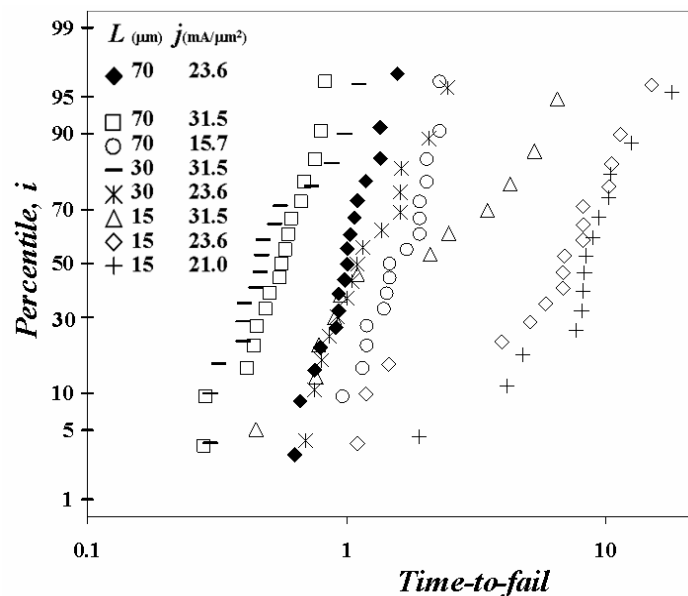


FIGURE 3. The distribution of the lifetime (DLT), measured from 8 groups of copper lines on the first wafer, tested at 300C. The time is scaled by t_* , the median time-to-fail of the group of the lines with $L = 70\mu\text{m}$ and $j = 23.6\text{mA}/\mu\text{m}^2$.

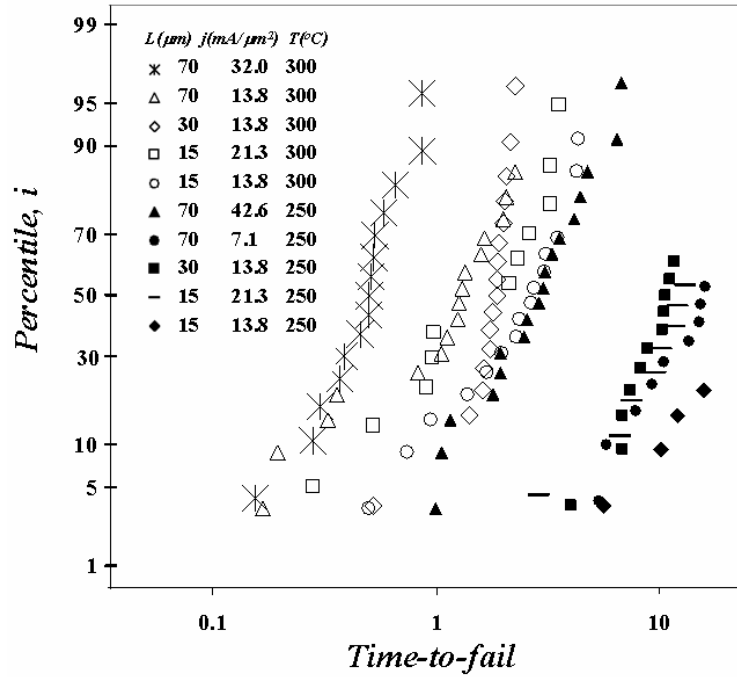


FIGURE 4. The distribution of the lifetime (DLT), measured from 5 groups of copper lines on the second wafer, and from 5 groups of copper lines on the third wafer, tested at 250C and 300C, respectively. The time is scaled by the same t_* as in Fig. 3. At this writing, many of the copper lines held at 250C have not failed, and the tests are still running.

Figure 4 shows the cumulative percentage frequency of the time-to-fail, measured from 5 groups of lines, on a second wafer, at temperature 250C, along with the data obtained from 5 groups of lines on a third wafer at temperature 300C. The electric current drives atoms to drift away from the via in the upper-level copper line (Fig. 2). The copper lines on the second and the third wafers have Design B.

THE VOLUME-TIME FUNCTION

In this section, we first review a transient model for electromigration in a metal line encapsulated in a dielectric. We then use the model to calculate the void volume as a function of time. Readers familiar with the model can skim this section, and focus on the final result, Eq. (9). Let the x -axis point in the direction of the electron flux. A void grows at the upstream via, $x = 0$. At time t , the stress in the line, $\sigma(x, t)$, is taken to be hydrostatic. According to Blech [9], both the electric current and the stress gradient drive the atomic flux:

$$J = \frac{D}{\Omega kT} \left(Z^* e \rho j + \Omega \frac{\partial \sigma}{\partial x} \right), \quad (1)$$

where J is the atomic flux, D the diffusion coefficient of atoms, Ω the volume per atom, k Boltzmann's constant, T the temperature, Z^* the effective valence, e the elementary charge, and ρ the resistivity.

As atoms drift in the line, some sections of the line gain atoms, and others lose. The total number of atoms in the line is conserved. Let θ be the volume fraction of atoms lost from a section of the line. This strain-like quantity relates to the stress as $\sigma = B\theta$, where B is an effective elastic modulus. Mass conservation requires that the rate at which a section loses atoms equal the divergence of the atomic flux: $\partial\theta/\partial t = \Omega\partial J/\partial x$. Combining the two relations with Eq. (1), Korhonen et al. [13] obtained that

$$\frac{\partial\sigma}{\partial t} = \frac{DB\Omega}{kT} \frac{\partial^2\sigma}{\partial x^2}. \quad (2)$$

This partial differential equation has the same form as the diffusion equation. The quantity $DB\Omega/kT$ serves the role of the diffusion constant. Dimensional considerations dictate that, for mass transport over the line length L , a characteristic time should be

$$\tau = (L^2kT)/(DB\Omega). \quad (3)$$

This characteristic time τ normalizes theoretical expressions.

We assume that the metal line spends its lifetime on growing the void, and neglect the time to nucleate the void. Before the electric current is applied, the stress in the line is negligible. After, the stress at the void is taken to be zero, and the atomic flux vanishes at the downstream via. These initial and boundary conditions, together with the partial differential equation (2), determine the stress $\sigma(x,t)$.

Once the stress field is solved, the void volume is calculated from the volume of atoms drifted into the line:

$$V = -A \int_0^L (\sigma/B) dx, \quad (4)$$

where A is the cross-sectional area of the line.

We now use this transient model to compute the void volume as a function of time. First consider the short-time, long-line limit: $t/\tau = t(DB\Omega)/(L^2kT) \rightarrow 0$. In this limit, the stress in the line has a negligible effect on the void volume, and Eq. (1) reduces to $J = DZ^*e\rho j/\Omega kT$. The void volume grows linearly with time, $V = \Omega J A t$, namely,

$$V = \frac{Z^*e\rho j D A t}{kT}, \quad \text{as } t/\tau \rightarrow 0. \quad (5)$$

This result has long been used to interpret the edge drift experiment [9]. If the failure time is reached when the void volume reaches a critical value, Eq. (5) reproduces a widely used empirical formula for the median-time-to-fail: $MTF = Cj^{-n} \exp(Q/kT)$, where C , n and Q are parameters to fit experimental data. Eq (5) identifies $n = 1$, and Q as the activation energy of diffusion. In this limit, the effective elastic modulus B plays no role.

Next consider the long-time, short-line limit: $t/\tau = t(DB\Omega)/(L^2kT) \rightarrow \infty$. In this limit, the line attains a steady state, in which the electron current balances the stress

gradient, and the atomic flux vanishes, $J = 0$. According to Eq. (1), the stress is linearly distributed along the line:

$$\sigma_{\text{sat}} = -\frac{Z^* e \rho j}{\Omega} x. \quad (6)$$

Inserting this stress distribution into Eq. (4), we obtain the saturated void volume:

$$V_{\text{sat}} = \frac{Z^* e \rho j L^2 A}{2 \Omega B}, \text{ as } t/\tau \rightarrow \infty. \quad (7)$$

This result has been used to study immortal interconnects [10-12]. For a line to be immortal, the void volume must be below a critical value. The saturated void volume is inversely proportional to the B . The effective elastic modulus is about 24 GPa when silica is used as the dielectric, and reduces to about 10 GPa when the carbon-doped oxide is used [3,5]. Everything else being equal, the saturated void volume in lines embedded in the compliant dielectric increases by a factor of 2. As mentioned above, this factor contributes to the mortality of the copper lines.

Finally consider the general transient state. The stress distribution $\sigma(x,t)$ is determined by solving Eq. (2), together with the initial and boundary conditions. The solution is a superposition of the steady-state stress distribution, Eq. (6), and a transient state. The latter is expressed as a series, determined by the method of separation of variables. The stress in the metal line as a function time is

$$\sigma(x,t) = -\frac{Z^* e \rho j L}{\Omega} \left\{ \frac{x}{L} + \frac{8}{\pi^2} \sum_n \frac{(-1)^n}{(2n-1)^2} \sin\left[\frac{(2n-1)\pi x}{2L}\right] \exp\left[-\left(\frac{2n-1}{2}\pi\right)^2 \frac{t}{\tau}\right] \right\}. \quad (8)$$

Figure 5 plots the stress distribution in the metal line at several times. As atoms diffuse downstream, compressive stresses arise in the line. The magnitude of the stress is small initially, and attains the linear distribution of the steady state in a long time.

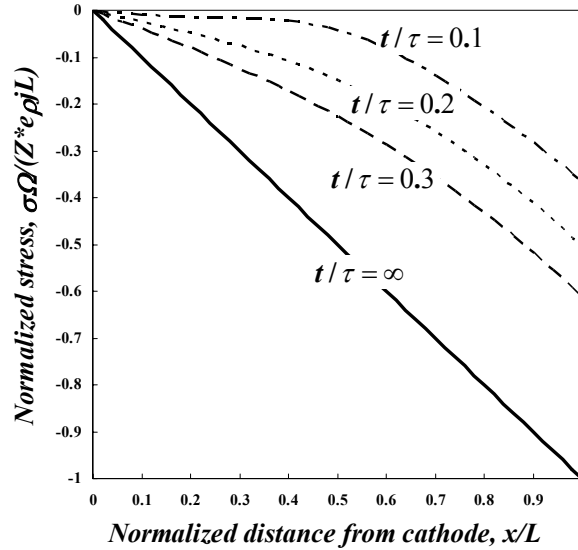


Figure 5 Stress distribution in a metal line at several times. A void exists at the cathode, $x = 0$, where the stress vanishes. As atoms drift into the line, a distribution of compressive stress builds up.

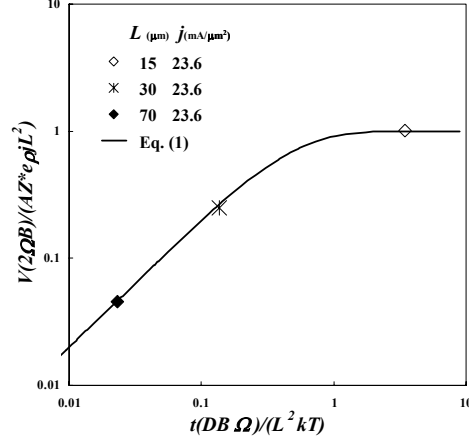


FIGURE 6. The void volume as a function of time, Eq. (9). The data points are the measured values of t_{50} for three groups of lines. By fitting the data points to the curve, we obtain a value of the parameter group $t_*DB\Omega/kT$.

Once the stress distribution is obtained, the integral in Eq. (4) gives the void volume as a function of time:

$$\frac{V}{V_{\text{satu}}} = 1 + \frac{32}{\pi^3} \sum_{n=1}^{\infty} \frac{(-1)^n}{(2n-1)^3} \exp\left[-\left(\frac{2n-1}{2}\pi\right)^2 \frac{t}{\tau}\right]. \quad (9)$$

The void volume is normalized by its saturated value $V_{\text{satu}} = (AZ^*ejL^2)/(2\Omega B)$, and the time by the characteristic time $\tau = (L^2kT)/(DB\Omega)$. Figure 6 plots the void volume as a function of the time. In the short-time, long-line limit, $t/\tau \rightarrow 0$, the void volume is linear in time. In the long-time, short-line limit, $t/\tau \rightarrow \infty$, the void attains the saturated volume, V_{satu} .

THE TWO-WAY CONVERSION BETWEEN DLT AND DVC

A substantial growth in the void volume involves atomic transport over the line length. The process averages over many copper grains along the line. Consequently, we expect that the void volume as a function of time, $V(t)$, is insensitive to chance variations of the microstructure. Specifically, we will use the deterministic equation (9) to relate the critical void volume and the time-to-fail. Let t_i be the time below which i percent of lines in a group fail, and V_i be the volume below which i percent of the critical voids lie. For a given set of testing variables, (L, j, T) , Eq. (9) provides a deterministic functional relationship between the two random variables t_i and V_i . Inverting Eq. (9), we can also write this function as

$$t_i = f(V_i; L, j, T). \quad (10)$$

One of our premises is that the DCV is independent of the testing variables (L, j, T) . For a given design, we can use Eq. (9) to obtain the DCV from the DLT measured under one set of (L, j, T) . We can then use the same DCV to predict DLT for lines of the same design under other sets of (L, j, T) according to Eq. (10).

To make the conversion between the two random variables t_i and V_i , we need to know material parameters that appear in Eq. (9). For each design, we first proceed to find a value of the parameter group $t_*DB\Omega/kT$. A set of experimental data $(t_{50}; j, L)$ can be plotted as a point on Fig. 6. For example, we plot three sets of data $(1; 23.6, 70)$, $(1.09; 23.6, 30)$ and $(6.87; 23.6, 15)$ obtained from the first wafer. On this log-log plot, a change in the parameters $t_*DB\Omega/kT$ and $(2V_{50}\Omega B)/(AZ^*e\rho)$ translates all the data points by the same amount. To fit the three points to the theoretical curve, we find that $t_*DB\Omega/kT = 1.12 \times 10^{-10} \text{ m}^2$ for Design A. By the same procedure, using data obtained from the third wafer, we obtain $t_*DB\Omega/kT = 1.10 \times 10^{-10} \text{ m}^2$ for Design B. The values for the two designs are nearly identical. This is expected, as the two designs share the same material set and integration process.

Figure 7 plots the DCV for Design A and Design B. For a given design, we obtain the DCV using the DLT measured from a single group of lines. For Design A, inserting the experimental values of t_i for the group for which $L = 70\mu\text{m}$ and $j = 23.6\text{mA}/\mu\text{m}^2$ into Eq. (9), and using the value of $t_*DB\Omega/kT$ obtained above, we obtain the corresponding values of $(2V_i\Omega B)/(AZ^*e\rho)$. For Design B, we obtain the DCV from the DLT of the group for which $L = 70\mu\text{m}$ and $j = 32.0\text{mA}/\mu\text{m}^2$ tested on the third wafer. Design B reduces the line width and the via diameter by about 30% from Design A. As expected, the critical void volumes in Design B are smaller than those in Design A.

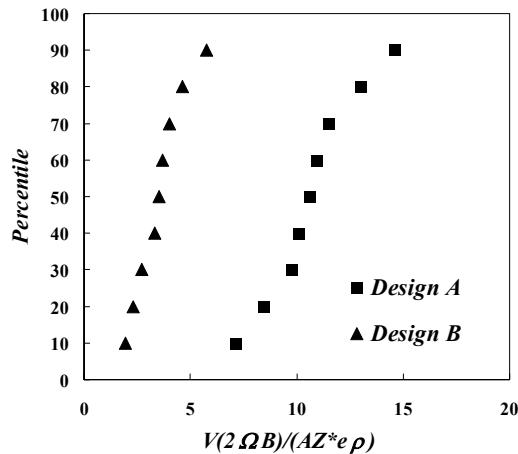


FIGURE 7. The distribution of the critical void volume (DCV). The parameter group has the same unit as the electric current, A.

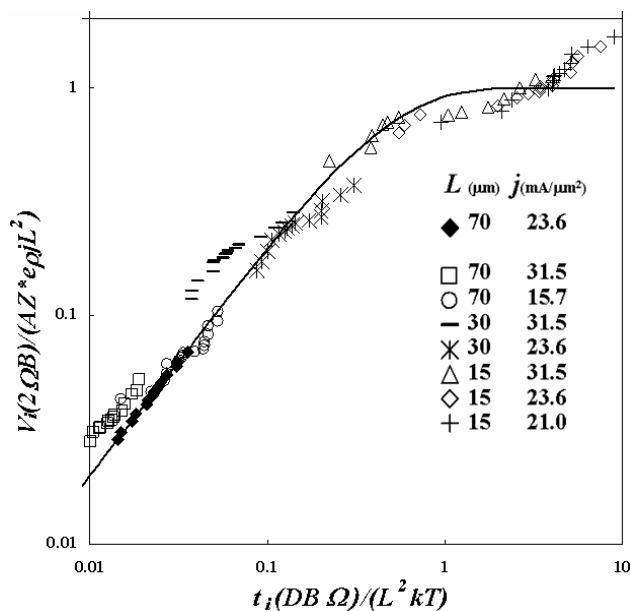


FIGURE 8. The curve, Eq. (9), provides a deterministic relation between the two random variables, V_i and t_i . Knowing V_i , the curve predicts t_i for given testing variables L and j . The theoretical curve is compared with the experimental values of t_i for the 8 groups of the copper lines on the first wafer.

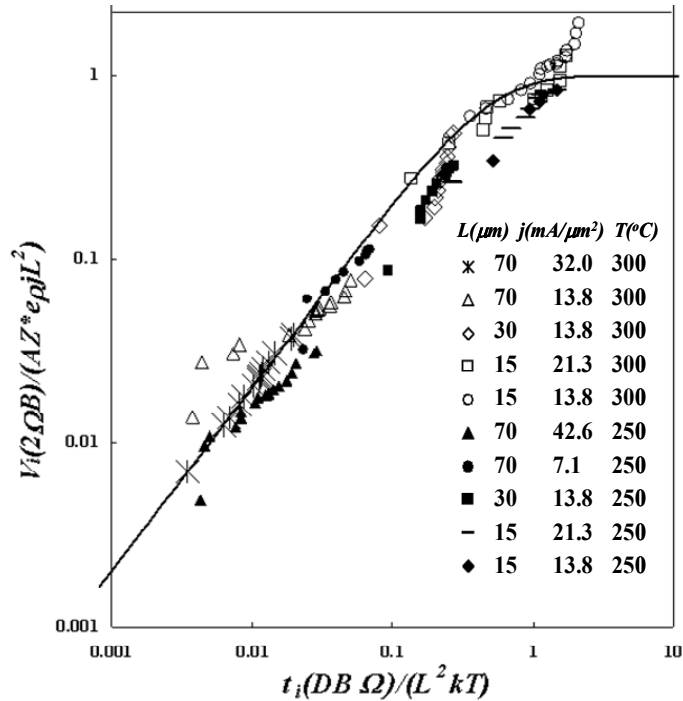


FIGURE 9. A comparison between the predicted times-to-fail with the measured ones for the 5 groups of the copper lines on the second wafer and the 5 groups of the copper lines on the third wafer.

The diffusion constants tested at the two temperatures are related by the Arrhenius equation $D = D_0 \exp(-Q/kT)$, where D_0 is the frequency factor, and Q the activation energy. The latter has been measured independently, $Q = 0.90$ eV. Once the DCV and the activation energy Q are known for a given fabrication process and line-end design, Eq. (10) predicts the DLT for any sets of the testing variables, j , L and T . Fig. 8 plots the experimental values of t_i for the lines of Design A against the values of V_i . Fig. 9 does the same for Design B. In the latter case, we have used the DLT measured on the third wafer tested at 300C, along with the activation energy, to predict the DLT on the second wafer tested at 250C. The agreement between the theoretical curve and the experimental data is encouraging, except for the short-line, long-time limit. The reason for this discrepancy is under investigation.

LIFETIME DISPERSION

Figure 6 indicates that the same variation in the critical volume causes a narrow lifetime dispersion for large j and L , but causes a wide lifetime dispersion for small j and L . This explains the trend of the experimental data in Figs. 3 and 4 and those reported by others [7]. From Eq. (9), a dimensionless measure of the lifetime dispersion, such as the sigma (the standard deviation of $\ln t_i$), is expected to be a function of jL^2 . Fig. 10 compares the predicted dispersion to the experimental data for the 8 sets of data of the first wafer. The agreement is again encouraging.

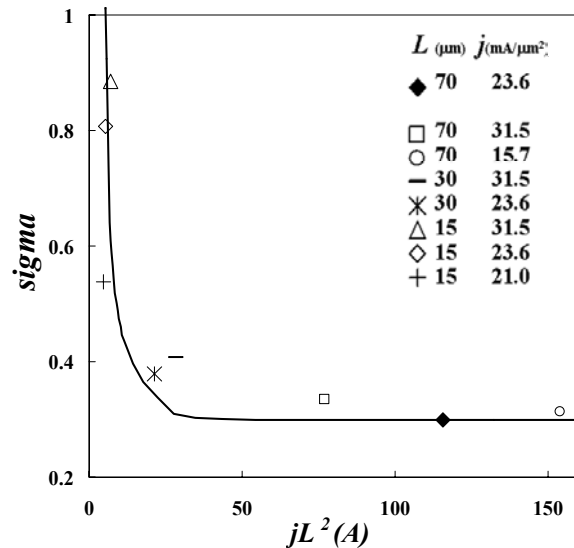


FIGURE 10. The standard deviation of $\ln t_i$, sigma, as a function of jL^2 . The data points are obtained from the 8 groups of lines reported in Fig. 3. The curve is plotted using Eq. (9), which predicts t_i from $t_i = f(V_i; L, j)$, using the values of V_i in Fig. 7.

SATURATED VOID VOLUME AND CRITICAL VOID VOLUME

Recall that the saturated void volume is given by $V_{\text{sat}} = (AZ^* e \rho j L^2) / (2\Omega B)$. If $V_{\text{sat}} = V_i$, the saturated void volume exceeds the critical volume of i percent of the lines. Consequently, $(jL^2)_i = (2V_i \Omega B) / (AZ^* e \rho)$ is the value of the jL^2 product below which i percent of the lines are mortal. Unfortunately, all the lines tested for this work are mortal, and our data do not fit well with the theoretical curve at the long-time limit (Fig. 8 and 9). Nonetheless, the three groups of the lines on the first wafer, tested at small values of jL^2 (4.73A, 5.18A, 7.01A), show large lifetime dispersion, indicative of approaching the immortality conditions. These jL^2 values are of the same order of magnitude as in Fig. 7.

Figure 7 gives the median critical volume V_{50} as $V_{50} / A = 145\text{nm}$ for the first wafer. (We take $\rho = 4.0 \times 10^{-8} \Omega\text{m}$, $\Omega = 1.18 \times 10^{-29} \text{m}^3$, $Z^* = 1.0$, and $B = 10\text{GPa}$.) This estimate falls in the range estimated by inspecting micrographs such as Fig. 1 and 2. We can estimate the critical volume from yet another consideration. For small voids, their shape is largely determined by the surface energy, and the electric current density is a weak driving force at this size scale. Copper atoms are mobile on the void surface. The void shape depends on the relative magnitude of the electron flux and the surface energy, as measured by the dimensionless number [14]

$$\eta = \frac{Z_s^* e \rho j a^2}{\gamma_s \Omega}, \quad (11)$$

where Z_s^* is the effective valence on copper surface, γ_s is the surface energy of copper, and a is the size of the void. For representative void size $a = 100\text{nm}$ and current density $j = 10^{10} \text{A/m}^2$, the dimensionless number is on the order $\eta = 10^{-1}$. Consequently, the void shape is largely determined by the surface energy. Neglect the anisotropy in the surface energy, and assume that the surface diffusion is fast compared to the transport along the line. The critical void takes the equilibrium shape of a spherical cap underneath the via, its base diameter coinciding with the via size d , giving the volume

Neglect the anisotropy in the surface energy, and assume that the surface diffusion is fast compared to the transport along the line. The critical void takes the equilibrium shape of a spherical cap underneath the via, its base diameter coinciding with the via size d , giving the volume

$$V_{\text{crit}} = \frac{\pi d^3}{12} \left(\frac{1}{1 - \cos \Psi} + \frac{\cos \Psi}{2} \right) \sin \Psi, \quad (12)$$

where Ψ is the wetting angle of copper on the liner. The critical volume increases as the wetting angle decreases. Taking $\Psi = 90^\circ$, $d = 250\text{nm}$ and $A \approx d^2$, we find that $V_{\text{crit}} / A = 98\text{nm}$. The three independent estimates give similar results, which provide a support for our approach.

In this paper, we have neglected the void volume due to thermal expansion mismatch between the copper lines and the surrounding materials. In particular, we

have used the DCV determined from a group of copper lines on the third wafer to predict DLT of lines on the second wafer. The two wafers are tested at 250C and 300C, respectively. The effect of thermal strain will be reported elsewhere.

CONCLUDING REMARKS

This paper analyzes the electromigration lifetime limited by voids grown at upstream vias. Our approach is based on two premises. First, the distribution of the critical void volume (DCV) is independent of the testing variables (j , L , T). Second, the functional relationship between the void volume and time is deterministic. Many sets of the distribution of lifetime (DLT) are obtained by testing copper lines on different wafers, subject to different values of the testing variables. We calculate the $V(t)$ function from a deterministic transient model. We then use $V(t)$ to obtain the DCV from a few sets of DLT. We finally use the same DCV to predict the DLT under other testing conditions. The agreement between the predictions and the experimental data demonstrates the merit of our premises and approach.

ACKNOWLEDGMENTS

The authors thank the process community at Intel for wafer fabrication and Michael McKeag for failure analyses. ZS acknowledges the financial support of the NSF MRSEC and the Division of Engineering and Applied Sciences at Harvard University.

REFERENCES

1. R. Rosenberg, D.C. Edelstein, C.-K. Hu, and K.P. Rodbell. *Annu. Rev. Mater.* 30, 229 (2000).
2. M.A. Hussein and Jun He, *IEEE Trans. Semicond. Manufact.* In press (2004).
3. S.P. Hau-Riege and C.V. Thompson, *J. Mater. Res.* 15, 1797 (2000).
4. K.-D. Lee, X. Lu, E.T. Ogawa, H. Matsushashi, P.S. Ho, 40th Ann Proc. IEEE Int Reliability Phys. Symp. pp. 322-326 (2002).
5. Z. Suo, pp. 265-324 in Volume 8: Interfacial and Nanoscale Failure (W. Gerberich, W. Yang, Editors), *Comprehensive Structural Integrity* (I. Milne, R.O. Ritchie, B. Karihaloo, Editors-in-Chief), Elsevier, Amsterdam, 2003.
6. S. P. Hau-Riege, *J. Appl. Phys.* 91, 2014 (2002).
7. C.S. Hau-Riege, A.P. Marathe, and V. Pham, 41st Ann Proc. IEEE Int Reliability Phys. Symp, IEEE, pp. 173-177 (2003).
8. C.-K. Hu, L. Gignac, E. Liniger, B. Herbst, D.L. Rath, S.T. Chen, S. Kaldor, A. Simon, and W.-T. Tseng, *Appl. Phys. Lett.* 83, 869 (2003).
9. I.A. Blech, *J. Appl. Phys.* 47, 1203 (1976).
10. R.G. Filippi, G.A. Biery, and R.A. Wachnik, *J. Appl. Phys.* 78, 3756 (1995).
11. Z. Suo, *Acta Mater.* 46, 3725 (1998).
12. V.K. Andleigh, V.T. Srikar Y.J. Park, C.V. Thompson. *J. Appl. Phys.* 86, 6737 (1999).
13. M.A. Korhonen, P. Boergesen, K.N. Tu, and C.-Y. Li, *J. Appl. Phys.* 73, 3790 (1993).
14. Z. Suo, W. Wang, and M. Yang, *Appl. Phys. Lett.* 64, 1944 (1994).